Jornadas de Automática

Modelling a wood fiber flash dryer for MDF production

Rasekhi, Saeed[a,*], Mazaeda, Rogelio[a], Tadeo, Fernando[a], Garcia Bombin, Angel[b]

[a] *Institute of Sustainable Processes, University of Valladolid, School of Industrial Engineering, Pso. Prado de la Magdalena 3-5, 47011 Valladolid, España.*

[b] SONAE ARAUCO, Calle Titulos, 29, 47009 Valladolid, España.

To cite this article: Rasekhi, Saeed, Mazaeda, Rogelio, Tadeo, Fernando, Garcia Bombin, Angel. 2025. Modelling a wood fiber flash dryer for MDF production. Jornadas de Automática, 46. https://doi.org/10.17979/ja-cea.2025.46.12115

Modelling a wood fiber flash dryer for MDF production

Resumen

Este trabajo presenta un modelo dinámico para el proceso de secado de fibra de madera en una línea de producción de tableros de fibra de densidad media (MDF). El modelo se centra en la etapa de secado convectivo dentro de un secadero tipo flash neumático, donde se intercambian humedad y calor entre las fibras en movimiento y la corriente de aire. Utilizamos un modelo unidimensional distribuido espacialmente para capturar la dinámica de transferencia de calor y masa. El modelo integra propiedades termo físicas del aire húmedo y las fibras húmedas, correlaciones empíricas no lineales y un coeficiente de secado dependiente de la humedad, inspirado en estudios previos. Implementado en Python, el sistema de ecuaciones diferenciales parciales se resuelve numéricamente mediante el método de líneas y el solucionador de backward-differentiation formulas. Este trabajo forma parte de una iniciativa amplia de gemelos digitales industriales en la Universidad de Valladolid, orientada a la detección de anomalías, la optimización energética y el análisis prescriptivo.

Palabras clave: Modelado de operaciones de manufactura, Simulación y Visualización, Modelado de caja gris, Implementación digital, Optimización de procesos.

Abstract

This work presents a dynamic model for the wood fiber drying process in a medium-density fiberboard (MDF) production line. The model focuses on the convective drying stage within a pneumatic flash dryer, where moisture and heat are exchanged between moving fibers and the air stream. We use a one-dimensional, spatially distributed model to capture heat and mass transfer dynamics. The model integrates thermophysical properties of humid air and wet fibers, nonlinear empirical correlations, and a humidity-dependent drying coefficient inspired by prior studies. Implemented in Python, the system of partial differential equations is numerically solved using the method of lines and the backward-differentiation formulas solver. This work is part of a broader industrial digital twin initiative at Universidad de Valladolid, aimed at anomaly detection, energy optimization, and prescriptive analytics.

Keywords: Modeling of manufacturing operations, Simulation and Visualization, Grey box modelling, Digital implementation, Process optimization.

1. Introduction

MDF production involves the washing and preheating process, mechanical defibration of wood chips into fibers with steam injection, followed by convective drying in a pneumatic dryer to reduce moisture content to optimal levels for resin application and hot pressing. The dryer is critical in product quality, process continuity, and energy efficiency.

Drying is inherently complex due to the nonlinear coupling of temperature, humidity, and airflow with fiber properties such as moisture content and specific heat. These complexities are magnified by changing operating conditions (e.g., feed rate, wood type, ambient air), motivating the development of a physically accurate model. Dried fibers at the outlet of the dryer will pass through a cyclone to separate wood fiber from air with a spiral movement, then it will be transferred to the

*Correspondence author: saeed.rasekhi@uva.es

Attribution-NonCommercial-ShareAlike 4.0 International (CC BY-NC-SA 4.0)

production line for pressing. There is another evaporation and moisture reduction throughout these steps. The preheating and defibration, and pressing processes are out of the scope of this article.

This work is part of an industrial digital twin project developed at Universidad de Valladolid. The larger goal includes real-time anomaly detection, performance assessment, quality prediction, and optimization.

In contrast to traditional black-box or lumped-parameter models, the proposed distributed-parameter model explicitly resolves the spatial dynamics of heat and mass transfer along the dryer using a set of coupled partial differential equations (PDEs). This allows accurate representation of axial temperature and humidity gradients, which are especially critical in capturing transitions between drying regimes, such as the shift from constant-rate to falling-rate phases. Lumped models, while computationally efficient, typically assume spatial homogeneity and fail to predict internal states critical for model-based control, particularly under transient or highly variable inlet conditions. By contrast, the present model integrates empirical correlations (e.g., Chilton–Colburn analogy, sigmoid-based drying kinetics) into a first-principles framework.

Compared to Pang's semi-empirical model (Pang, 2001), which discretizes the dryer in space but treats drying kinetics using piecewise-constant parameters, our model introduces a continuous nonlinear drying coefficient $\alpha(Hf)$ using sigmoid functions. This eliminates artificial phase transitions between constant- and falling-rate regimes, improving both numerical stability and physical realism. Moreover, our model expands Pang's framework by explicitly including pipe wall dynamics, humidity-dependent air properties, and mass transfer correlations derived from Chilton–Colburn analogies, enabling broader applicability across operational ranges.

2. Methodology

We model the dryer as a one-dimensional convective flow system for gas-solid interactions, discretized along its length. The states are fiber temperature, fiber humidity, air temperature, air humidity, and pipe wall temperature. The model resolves energy and mass balances at each segment using finite volume techniques.

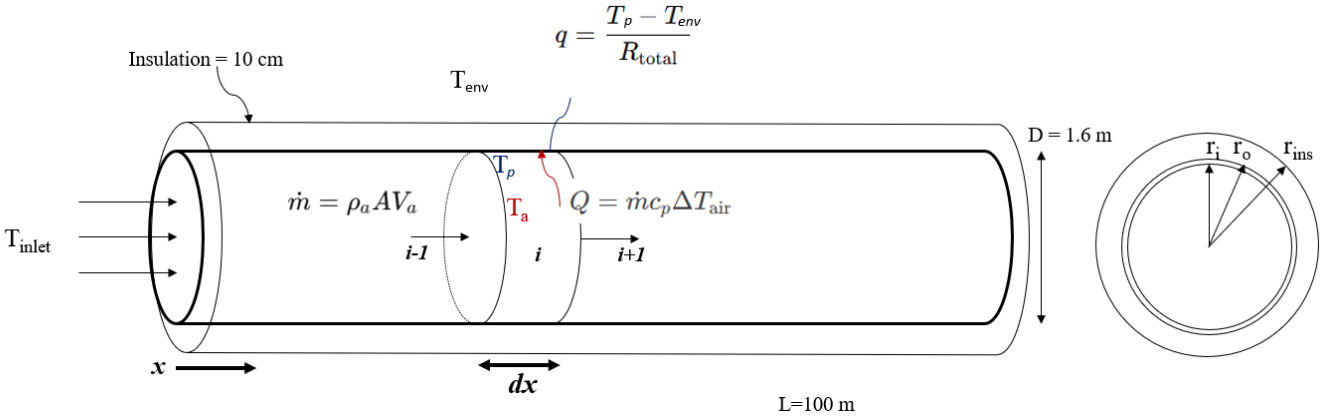

Figure 1: Schematic of Dryer tube, the segment of length.

Figure 1 represents a schematic of the convective drying tube used for modelling the airflow and heat exchange in an MDF fiber dryer. Air enters at the inlet with a known temperature T_inlet and flows axially through a cylindrical steel pipe of length L=100 meters and diameter D=1.6 meters. The mass flow rate of air is described by $\dot{m} = \rho_a * A * V_a$, where ρ_a is the air density, A is the cross-sectional area, and V_a is the bulk air velocity. Along the tube, differential control volumes of size dx are considered for spatial discretization. At each segment i, air exchanges heat with the steel wall (pipe surface temperature T_p) and loses energy to the surroundings through conduction across the pipe and insulation. The heat transfer rate from the steel pipe to the insulation, and from the insulation to the outside ambient air, are considered as constant values. The total thermal resistance is equal to pipe resistance plus insulation resistance plus external resistance. The radial heat loss to the environment is modelled using the thermal resistance concept ($R_{totlal,}$ the total thermal resistance including the steel wall and 10 cm thick insulation). This dual mechanism of convective axial heat transfer and radial heat loss is essential for modelling realistic transient behavior and energy efficiency in the drying process. The pipe cross-section on the right illustrates the layered structure defined by the internal radius r_i, outer wall radius r_o, and the insulation boundary at r_{ins}.

2.1. Mass and Energy Balance

The model describes the dynamic behavior of heat and mass transfer between moving air and wood fibers in a one-dimensional convective drying process. The system consists of five coupled PDEs representing:

Fiber humidity loss due to evaporation, models evaporation of water from fiber to air, and includes a nonlinear drying rate coefficient α(Hf):

$$\frac{dH_f}{dt} = -\alpha(H_f) \times k_{evap} \times \frac{H_f - H_a}{\dot{m}_f} - v_f \times \frac{\partial H_f}{\partial x} \qquad (1)$$

Air humidity increases due to the fiber's evaporation, tracks moisture gain in air from the evaporated fiber moisture, and is coupled to fiber drying dynamics:

$$\frac{dH_a}{dt} = -\beta \times \frac{\rho_f \times v_f}{\rho_a \times v_a} \times \frac{dh_f}{dt} - v_a \times \frac{\partial H_a}{\partial x} \quad (2)$$

Fiber temperature dynamics include convective heating from air and cooling from evaporation, and the latent heat effects are explicitly modelled:

$$\frac{dT_f}{dt} = \frac{h_{af} \times A_f}{\rho_f \times C_{p,f}} \times \left(T_a - T_f\right) + \frac{H_{wv}}{C_{p,f}} \times \frac{dH_f}{dt} - v_f \times \frac{\partial T_f}{\partial x} \quad (3)$$

Air temperature dynamics, air loses energy to the fiber and to vaporize moisture, sensitive to transient fiber behavior:

$$\frac{dT_a}{dt} = -\beta \times \frac{\rho_f \times v_f}{\rho_a \times v_a \times C_{p,a}} \times \left(C_{p,f} \times \frac{dT_f}{dt} - H_{wv} \times \frac{dH_f}{dt}\right) - v_a \times \frac{\partial T_a}{\partial x} \quad (4)$$

Dryer tube wall thermal dynamics models heat accumulation in the metal wall and loss to ambient, and provides boundary interaction between airflow and the surrounding system:

$$\frac{dT_p}{dt} = \frac{1}{C_{pipe}} \times \left(h_{ap} \times P_{pipe} \times \left(T_a - T_p\right) - \frac{T_p - T_{env}}{R_{total}}\right) \quad (5)$$

These equations are nonlinear, coupled, and convective-dominant, making them representative of real industrial dryers. They are discretized using the method of lines and solved as a system of ODEs in time.

2.2 Physical and Empirical Correlations

We are widely using empirical formulas from the literature to create a more accurate dynamic model of the flash dryer, which includes characteristics of air and wood fiber that depend on temperature and humidity.

Table 1 lists all the Parameters used in the calculations, including the physical characteristics of the air, wood fiber, and steel pipe.

Table 1: Physical parameters

Symbol	Description	Units
T_f	Fiber temperature	K (Kelvin)
H_f	Fiber moisture	kg water/kg dry fiber
T_a	Air temperature	K (Kelvin)
H_a	Air specific humidity	kg water/kg dry air
T_p	Pipe wall temperature	K (Kelvin)
ρ_a	Density of air	kg/m³
ρ_f	Density of fiber	kg/m³
Cp_a	Specific heat capacity of air	J/kg·K
Cp_f	Specific heat of fiber	J/kg·K
μ_a	Dynamic viscosity of air	Pa·s (kg/m·s)
k_a	Thermal conductivity of air	W/m·K
D_a	Diffusivity of water vapor in air	m²/s
h_{af}	Convective heat transfer coefficient (air–fiber)	W/m²·K
h_{ap}	Convective heat transfer coefficient (air–pipe)	W/m²·K
k_{evap}	Evaporation mass transfer coefficient	kg/s
kc	Mass transfer velocity	m/s
$\alpha(H_f)$	Drying coefficient	— (dimensionless)
$\dot{m}$	Mass flow rate of air	kg/s
Va	Velocity of air	m/s
v_f	Velocity of fiber	m/s
A	Cross-sectional area of pipe	m²
A_f	Effective area of fiber-air contact	m²
R_{total}	Total radial thermal resistance from air to ambient	K/W
H_{wv}	Latent heat of evaporation	J/kg
Pr	Prandtl number of air	—
Sc	Schmidt number of air	—
Re	Reynolds number of the flow	—
Nu	Nusselt number	—
β	Effective volumetric ratio	—
C_{pipe}	Pipe thermal capacitance	J/K

The density of the humid air is calculated by $\rho_a = \frac{P}{R_{air} \times T} \times \frac{1}{1+1.6078 \times H_a}$ (Moran et al., 2010) (ASHRAE, 2017). The specific heat of humid air and specific heat of water vapor, and latent heat for evaporation were calculated by implicit formulas (Incropera et al, 2007).

The dynamic viscosity of air and the diffusivity of water vapor in air, and the thermal conductivity of air are taken from the implicit formula (Reid et al., 1987).

The Reynolds number (to calculate heat transfer between air and fiber) will be $Re = \frac{\rho_a \times D_h \times (v_a - v_f)}{\mu_a}$, were the hydraulic diameter of the fiber is defined by $D_h = 2 \times \frac{d_f \times l_f}{d_f + l_f}$, and the velocity slip between air and fiber is $v_f = v_a \times (1 - 0.0639 \times d_f^{0.3} \times \rho_f^{0.5})$ (Perry and Green, 1984), (Pang, 2001). This empirical slip relation is used in particle transport modelling for fiber-air dynamics.

Convective heat transfer coefficient (between air and fiber) is defined by $h_{af} = \frac{N_u \times k_a}{d_f}$, where the Nusselt number and the Schmidt number are obtained from (Churchill and Bernstein, 1977), and the Prandtl number by $P_r = \frac{\mu_a \times C_{p,a}}{k_a}$ (Incropera et al., 2007).

The Chilton-Colburn mass transfer coefficient k_{evap}, is widely used in chemical engineering for estimating mass transfer coefficients in convective processes (Bird et al., 2002).

Convective heat transfer coefficient (between air and pipe wall) calculated by $h_{ap} = N_u \times \frac{k_a}{d_{pipe}}$, where $P_r = 0.7$, and $N_u = 0.023 \times Re^{0.8} \times \mathrm{P_r}^{0.3}$ using the Churchill-Bernstein equation.

Thermophysical properties ($C_{p,a}$, $C_{p,f}$, ρ_a, μ_a , k_a , D_a) are obtained using tabulated correlations from literature (Dietenberger, 2002), (ASHRAE, 2017).

The drying rate coefficient (α) acts as a tuning parameter for considering different conditions of water evaporation from the wood fibers (Pang, 2001):

- When the moisture content is higher than 50%, the liquid water evaporates at the fiber surface, while the liquid water within the fiber moves outwards to the surface. In this stage, the drying rate is high and relatively constant.
- If the moisture content is between 20 and 50%, the fiber surface is no longer saturated, and moisture evaporates within the material. The evaporated vapor first flows through the fiber and then diffuses into the airstream. The drying rate decreases in this stage of drying.
- Finally, when the moisture content is below 20%, only bound water and water vapor exist. During this stage, the drying is controlled by bound water diffusion and vapor flow within the fiber walls, and thus, the drying rate is very low.

The drying rate coefficient used in this work is a nonlinear empirical function of the fiber moisture content (H_f). It is designed to capture two key drying phases:

- Constant-rate phase: rapid evaporation when the fiber surface is saturated.
- Falling-rate phase: evaporation slows as bound water diffuses from inside the fiber.

Our model generalizes this concept using $\alpha(\mathrm{H_f})$, allowing flexible, tenable drying kinetics suitable for different fiber types and operating conditions. The sigmoid approach improves numerical robustness and realism in later drying stages, where moisture levels are low and traditional linear assumptions fail. Drying coefficient is a sigmoid function as $\alpha(H_f) = 0.023 + 0.712 \times \sigma(H_f, k = 50, x_0 = 0.5) + 0.265 \times \sigma(H_f, k = 50, x_0 = 0.2)$. The nonlinear drying kinetics modelling is based on saturation behaviour described by Pang.

2.3. Numerical Solution

The system of PDEs is solved by discretizing them in space (method of lines), producing a system of ODEs. The Method of Lines (MoL) is selected due to its compatibility with stiff solvers and ease of coupling nonlinear boundary conditions. While Finite Difference (FDM) or Finite Element Methods (FEM) could also be used, MoL provides sufficient accuracy and computational efficiency for one-dimensional convective-dominant systems of this type. Integration is carried out using the backward-differentiation formulas (BDF) method over time. Material properties are dynamically updated at each step based on empirical correlations. The spatial discretization is implemented by dividing the length of the dryer into 100 points, and for the cyclone into 50 points. The calculation timestep is considered as 1 second, from time zero to 1000 seconds. First-order upwind finite difference schemes are applied to the convective terms, given the dominance of convective transport, and to ensure numerical stability.

One of the key aspects of the simulation is the calculation time, which in our case is around 1.7 seconds. Due to the residence time in the flash dryer, which is around 3-4 seconds, the calculation should be continuously updated based on real-time measurements of the real plant data, to be able to be implemented for NMPC. In this case, the calculation time of the model is less than the residence time in the dryer.

3. Results and Discussion

The final state of the dynamic model is presented in Figure 2, demonstrating the Temperature and the Humidity.

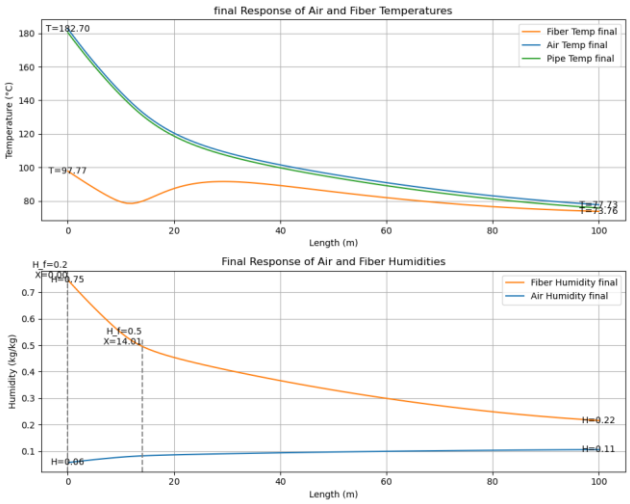

Figure 2: Final state of temperature and moisture of the dynamic model of the flash dryer. the steady-state profiles of temperature (top) and humidity (bottom) along the length of the fiber dryer (from 0 to 100 meters)

As shown in Figure 2, the air enters the dryer at a temperature of approximately 187 °C and progressively loses heat to the cooler fiber and dryer tube steel pipe wall. The fiber temperature begins near 100 °C and drops quickly to below 80 °C in the first section before gradually increasing to near 90 °C and falls again below 70 °C. While the most intense exchange occurs in the first 20–30 meters of the dryer, the fiber starts with a high humidity content of 0.77 kg/kg and undergoes significant moisture reduction, falling below 0.5 kg/kg, and reaching 0.2 kg/kg at the outlet. The initial steep decline indicates the high drying phase dominated by surface evaporation. Air humidity increases from 0.06 to 0.11 kg/kg due to moisture absorption, but its growth rate slows depending on α. These trends confirm the model's ability to capture coupled heat and mass transfer processes along the drying tunnel.

Along with the flash dryer model, the dynamic model of the Cyclone is presented. In the cyclone, the wood fibers and air are separated due to the decreasing velocity of the wood fibers falling from the top to the bottom in a spiral movement. We modified the dryer model to simulate the water evaporation in the cyclone by implementing the physical behavior of gas-solid separation by drag force between air and fibers. Instead of considering a slip velocity (as in the dryer

model), it is considered that the drag force will affect the velocity of fibers. This simulation was done separately with the same method of calculation, the initial conditions are taken from the dryer outlet, and the final state of this model is presented in Figure 3.

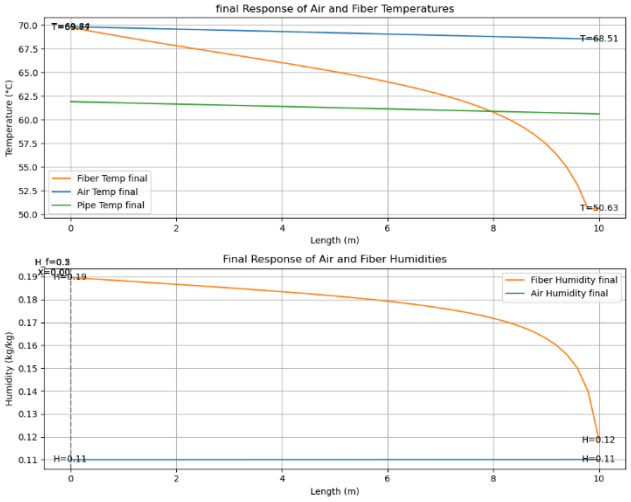

Figure 3: Final state of Temperature and Humidity of the dynamic model of Cyclone. The steady-state profiles of temperature (top) and humidity (bottom) along the height of the cyclone (0 at top, and 10 at the bottom)

During the separation process in the cyclone, the velocity of wood fibers decreases exponentially from top to bottom, which respectively affects the Reynolds number and increases the humidity transfer rate. While the temperature of the air remains above 60 °C, the fiber enters with a moderate humidity of 0.19 kg/kg and reaches around 0.12 kg/kg by the bottom of the cyclone. The air humidity increases slightly from 0.11 to 0.12 kg/kg, confirming limited moisture transfer due to the constrained drying length.

3.1. Effect of Fiber Size

Larger diameter fibers exhibit slower moisture diffusion, requiring higher or extended residence time. This is reflected in lower Re numbers and mass transfer coefficients.

The simulated profiles verify expected physical behavior:

- Air temperature decreases along the tube due to energy transfer to the fibers and the dryer tube steel pipe wall.
- Humidity increases and flattens as equilibrium approaches.

3.2. Heat exchange with dryer tube wall

Thermal inertia of the dryer tube is significant under transient startup or shutdown conditions. Inclusion of the dryer tube wall equation improves temperature lag estimation and prevents underestimation of drying time. The heat transfer between air and the steel tube, and the heat loss to the environment through an insulation layer, was added to the model.

3.3. Dynamic behavior of the model

At the onset of operation, the model captures a distinct preheating phase, during which the steel pipe wall, initially at ambient temperature, absorbs heat from the hot inlet air. This thermal inertia delays the rise in air temperature along the dryer length, as a significant portion of the convective heat is initially stored in the wall. As a result, the effective heat transfer to the fibers is reduced during the first few seconds or minutes of startup. This lag is especially evident in the fiber temperature and moisture profiles, which remain nearly unchanged until the wall temperature approaches a steady state. This behavior emphasizes the importance of including the pipe wall dynamics in the model, as it directly affects early moisture removal efficiency and startup stability. The preheat time evolution to warm up the dryer tube steel pipe is approximately 10-15 minutes from 20 to 180 °C (based on the data from the production line), as demonstrated in Figure 4.

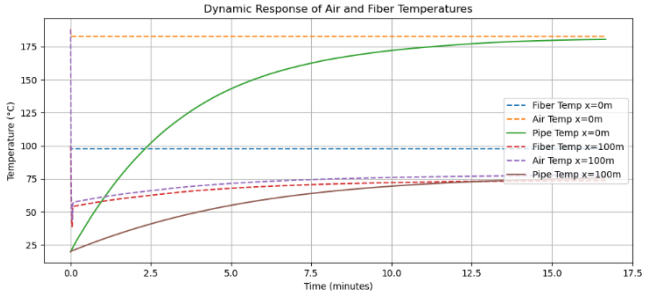

Figure 4: Dynamic behavior of the flash dryer model. Temperature of air, fiber, and pipe at x=0 and x=100 m.

4. Conclusion

We have developed and implemented a detailed first-principles model of a pneumatic wood fiber dryer. The model integrates spatially distributed heat and mass balances, humidity-driven evaporation kinetics, and real thermophysical properties of air and wood. An important feature of the model is the use of a nonlinear sigmoid-based drying coefficient, which enhances numerical stability and realism during both constant-rate and falling-rate drying phases. The inclusion of wall thermal dynamics further improves realism under transient conditions such as startups and disturbances.

The model is implemented using a method-of-lines approach in Python and is suitable for simulation, digital twin deployment, and advanced control design. Its structure supports integration with real-time optimization, parameter estimation, and anomaly detection frameworks. As part of a larger industrial digital twin initiative, this model lays the foundation for predictive control strategies and data-driven decision-making in energy-intensive MDF processes.

Although this work does not include parameter estimation, the model structure is compatible with parameter fitting techniques when experimental or plant data are available. For instance, key parameters such as the drying coefficient α(H_f), convective heat transfer coefficients h_af, and fiber-specific properties could be estimated via nonlinear least-squares optimization methods such as Levenberg–Marquardt or global metaheuristics. These methods can be combined with physical parameter bounding and regularization to enhance robustness and prevent overfitting. Integrating these techniques is part of our planned future work, aimed at adapting the model to plant-specific behavior and supporting digital twin applications. Future work will focus on experimental validation, model

reduction for real-time use, and integration into nonlinear model predictive control (NMPC) platforms to enhance process efficiency, product quality, and sustainability.

Acknowledgements

This work is part of the Project WISEBRAIN (CPP2021-008639), funded by MICIU/AEI/10.13039/501100011033 and NextGenerationEU and by Universidad de Valladolid.

References

ASHRAE, 2017. *ASHRAE handbook – fundamentals*. American Society of Heating, Refrigerating and Air-Conditioning Engineers, Atlanta, GA.

Bejan, A., Kraus, A. D., 2003. *Heat transfer handbook*. Wiley, Hoboken, NJ.

Bird, R. B., Stewart, W. E., Lightfoot, E. N., 2002. *Transport phenomena*, 2nd ed. Wiley, New York.

Churchill, S. W., Bernstein, M., 1977. A correlating equation for forced convection from gases and liquids to a circular cylinder in crossflow. *Journal of Heat Transfer* 99(2), 300–306. https://doi.org/10.1115/1.2134480

Dietenberger, M. A., 2002. A comprehensive model for the thermophysical properties of wood. *Wood and Fiber Science* 34(4), 690–703.

G. D. Byrne, A. C. Hindmarsh, 1975. A Polyalgorithm for the Numerical Solution of Ordinary Differential Equations. ACM Transactions on Mathematical Software, Vol. 1, No. 1, pp. 71-96.

Incropera, F. P., DeWitt, D. P., 2007. *Fundamentals of heat and mass transfer*, 6th ed. Wiley, Hoboken, NJ.

Moran, M. J., Shapiro, H. N., 2010. *Fundamentals of engineering thermodynamics*, 7th ed. Wiley, Hoboken, NJ.

Pang, S., 2001. Improving MDF fiber drying operation by application of a mathematical model. *Drying Technology* 19(8), 1789–1805. https://doi.org/10.1081/DRT-100107273

Perry, R. H., Green, D. W., 1984. *Perry's chemical engineers' handbook*, 6th ed. McGraw-Hill, New York.

Reid, R. C., Prausnitz, J. M., Poling, B. E., 1987. *The properties of gases and liquids*, 4th ed. McGraw-Hill, New York.

Santos, P., Pitarch, J. L., de Prada, C., 2019. Energy-efficient operation of a medium-density fibreboard dryer through nonlinear MPC. *IFAC-PapersOnLine* 52(1), 400–405. https://doi.org/10.1016/j.ifacol.2019.06.093

Santos, P., Pitarch, J. L., Vicente, A., de Prada, C., García, Á., 2020. Improving operation in an industrial MDF flash dryer through physics-based NMPC. *Control Engineering Practice* 94, 104213. https://doi.org/10.1016/j.conengprac.2019.104213

VDI, 2010. *VDI Heat Atlas*, 2nd ed. Springer-Verlag, Berlin.

White, F. M., 2006. *Viscous fluid flow*, 3rd ed. McGraw-Hill, New York.